JOURNAL OF THE KOREAN ASTRONOMICAL SOCIETY
36: S37 ~ S44, 2003

MAGNETIC HELICITY CHANGES OF SOLAR ACTIVE REGIONS BY PHOTOSPHERIC HORIZONTAL MOTIONS

Y.-J. MOON[1,2], JONGCHUL CHAE[1,3], AND Y. D. PARK[2]
[1] Big Bear Solar Observatory, NJIT, 40386 North Shore Lane, Big Bear City, CA 92314, USA
E-mail: yjmoon@bbso.njit.edu
[2]Korea Astronomy Observatory, Whaamdong, Yooseong-ku, Daejeon, 305-348, Korea
[3] Department of Astronomy and Space Science, Chungnam National University, Daejeon 305-764, Korea

ABSTRACT

In this paper, we review recent studies on the magnetic helicity changes of solar active regions by photospheric horizontal motions. Recently, Chae(2001) developed a methodology to determine the magnetic helicity change rate via photospheric horizontal motions. We have applied this methodology to four cases: (1) NOAA AR 8100 which has a series of homologous X-ray flares, (2) three active regions which have four eruptive major X-ray flares, (3) NOAA AR 9236 which has three eruptive X-class flares, and (4) NOAA AR 8668 in which a large filament was under formation. As a result, we have found several interesting results. First, the rate of magnetic helicity injection strongly depends on an active region and its evolution. Its mean rate ranges from 4 to 17 $\times 10^{40}$ Mx^2 h^{-1}. Especially when the homologous flares occurred and when the filament was formed, significant rates of magnetic helicity were continuously deposited in the corona via photospheric shear flows. Second, there is a strong positive correlation between the magnetic helicity accumulated during the flaring time interval of the homologous flares in AR 8100 and the GOES X-ray flux integrated over the flaring time. This indicates that the occurrence of a series of homologous flares is physically related to the accumulation of magnetic helicity in the corona by photospheric shearing motions. Third, impulsive helicity variations took place near the flaring times of some strong flares. These impulsive variations whose time scales are less than one hour are attributed to localized velocity kernels around the polarity inversion line. Fourth, considering the filament eruption associated with an X1.8 flare started about 10 minutes before the impulsive variation of the helicity change rate, we suggest that the impulsive helicity variation is not a cause of the eruptive solar flare but its result. Finally, we discuss the physical implications on these results and our future plans.

Key words : Sun: magnetic fields—Sun: flare—Sun: filament—Sun: coronal mass ejection—Sun: photosphere

I. INTRODUCTION

There have been many reports on the helical structures of solar and heliospheric magnetic fields; for example, photospheric magnetic fields (Pevtsov & Canfield 1999), coronal X-ray images (Canfield & Petsov 1999), solar filaments (Chae 2000), coronal mass ejections (Rust 1999), and interplanetary magnetic fields (Burlaga 1988). So far most observational studies of the helicity in solar active regions have focused on the current helicity, defined as $\int \boldsymbol{B} \cdot \boldsymbol{J}\, dV$, and its sign (or the linear force-free coefficient α), mainly because they can be directly inferred from photospheric vector magnetograms (Pevtsov & Canfield 1999). The current helicity is a measure of the topological properties such as twist and mutual linkages of the lines of electric current. On the other hand, magnetic helicity, defined as $\int \boldsymbol{A} \cdot \boldsymbol{B}\, dV$, is a measure of twist and linkage of magnetic field lines (DeVore 2000). The magnetic helicity is a physically more useful concept than the current helicity, because magnetic helicity is fairly well-conserved in a closed volume. So it is considered as a robust invariant in space plasmas such as the solar corona. However, the magnetic helicity has rarely been measured because of the difficulty in determining the topological connection of field lines in a 3D space. Instead, there have been efforts to determine its rate in an open volume.

Since the solar corona is an open volume with the photosphere as a boundary with normal flux, the magnetic helicity can be transported across the boundary by velocity fields in the photosphere. According to Berger & Field (1984), the Poynting theorem for magnetic helicity in an open volume is given by

$$\frac{dH}{dt} = 2 \oint (\boldsymbol{B} \cdot \boldsymbol{A}_\mathrm{p}) v_z \, dS - 2 \oint (\boldsymbol{v} \cdot \boldsymbol{A}_\mathrm{p}) B_z \, dS \,, \quad (1)$$

where $\boldsymbol{A}_\mathrm{p}$ is the unique vector potential of the potential field satisfying the following conditions:

$$\nabla \times \boldsymbol{A}_\mathrm{p} \cdot z = B_z, \ \nabla \cdot \boldsymbol{A}_\mathrm{p} = 0, \ \boldsymbol{A}_\mathrm{p} \cdot z = 0. \quad (2)$$

Eq.(1) tells that the magnetic helicity in an open volume can change either by the passage of field lines

Corresponding Author: Y.-J. Moon

through the surface (first term, which is called advection term) or by the horizontal motions of field lines (second term or shear term). Recently, Chae (2001) developed a direct method of deriving the shear term from observations.

We have applied this methodology to several active regions associated with solar flares and filaments: (1) NOAA AR 8100 which has a series of homologous X-ray flares (Moon et al. 2002a, Paper I), (2) three active regions which have four eruptive major X-ray flares(Moon et al. 2002b, Paper II) (3) NOAA AR 9236 which has three eruptive X-class flares (Moon et al. 2003, Paper III) and (4) NOAA AR 8668 in which a large filament was under formation (Chae et al. 2001, Paper IV). For this we have used 1-min cadence SOHO/MDI (Scherrer et al. 1995) longitudinal magnetograms. In this paper we review the main results of these applications together with other related studies and discuss their physical implications.

II. DATA ANALYSIS

To determine the second term of Eq.(1), we need three physical quantities: longitudinal magnetic field, vector potential of the potential field, and horizontal velocity vector. For the estimation of these quantities, we have used sets of MDI 1 minute full-disk or high resolution longitudinal magnetograms. The field of views of magnetograms that we analyze were taken to cover the whole active regions under consideration. The noise level in the 1-min cadence data is found to be about 10 G per pixel from a comparison of two successive magnetograms. All the magnetograms were aligned by the non-linear mapping, which takes into account the solar differential rotation effect (Chae et al. 2001). This procedure is also effective in correcting for the geometrical foreshortening originating from the spherical geometry of the Sun. To increase the signal-to-noise ratio, we have taken time averages by adopting median values of five successive magnetograms. Since the active regions under consideration for most cases were located near solar disk center during the observations, the effects of off-center projection should be regarded to be small. A detailed quantitative discussion on the effects was given in Paper IV. Detailed procedures for data analysis were well described by Chae(2001) and Paper I.

The horizontal velocity field has been determined from the lateral displacement of magnetic flux concentrations using local correlation tracking method (hereafter, LCT) described in November & Simon (1988). For the LCT, there are two important input parameters: FWHM of the apodization window and the time interval between two images for comparison. We select the FWHM of 8″, four times the spatial sampling size of the MDI full disk data. The time interval for horizontal velocity measurement is set to 20 minutes, which corresponds to about 0.34 pixels when a magnetic flux element moves with a speed of 0.2 $\mathrm{km\,s^{-1}}$. To reduce the contribution of noises, we set to zero the

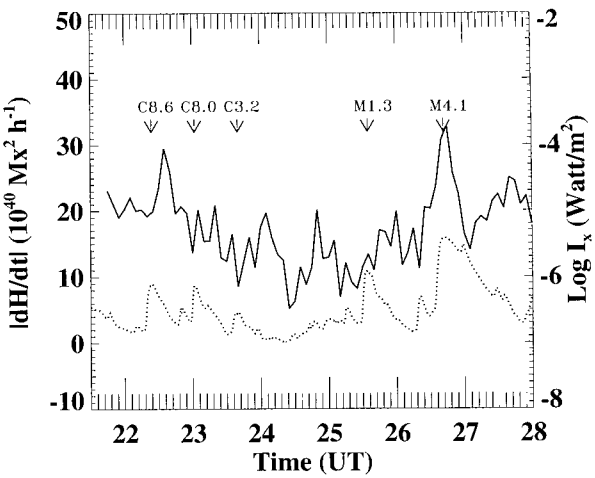

Fig. 1.— Temporal evolution of the magnetic helicity rate (solid line) by horizontal photospheric motions and the GOES intensity (dotted line) in 1-8 Å bands. The GOES intensity is referenced to the right vertical axis and the arrows indicate the X-ray intensity peak of homologous flares.

horizontal velocity in the regions with low flux densities (less than 10 G) or low cross-correlation value (less than 0.9). The criterion of a high correlation value is made for preventing from unrealistic variations such as the change of spectral lines associated with flaring process. Vector potential $\mathbf{A}_\mathrm{p}$ of the potential field is determined using the Fourier transform method described in Chae(2001). To minimize the effect of a periodic boundary condition in the computation of $\mathbf{A}_\mathbf{p}$, we employed 2D computational boxes that are several times as large as the regions of interest.

III. MAGNETIC HELICITY INJECTION

(a) Helicity Injection Rate

Figure 1 shows the temporal variation of magnetic helicity change rate of NOAA AR 8100 for 6.5 hours (Paper I). In this active region, there were a series of homologous flares during the period (Table 1 of Paper I). The magnetic helicity injected by shear flows for the period is $\Delta H = 1 \times 10^{42}$ Mx^2 and its mean helicity injection rate is about $| < dH/dt > | = 1.7 \times 10^{41}$ Mx^2 h^{-1}. Table 1 summarizes major characteristics of the magnetic helicity injections by photospheric horizontal motions from several literatures including our four papers (Paper I-IV). Except for the first case having no flare event, the absolute value of mean helicity injection rate ranges from 4 to 17 $\times 10^{40}$ Mx^2 h^{-1}. All of these events were associated with solar eruptive events such as solar flares and coronal mass ejections (CMEs). It is hard to estimate the portion of the magnetic helicity contribution by shear flows as given in Table 1 in the total

TABLE 1
SUMMARY OF MAGNETIC HELICITY INJECTION BY PHOTOSPHERIC HORIZONTAL MOTIONS.

Date	NOAA AR	Period (hr)	ΔH (10^{40}Mx^2)	$< dH/dt >$ (10^{40}Mx^{2}h^{-1})	Related Events	Reference
1997 Jan. 17	8011	39	0.7	0.02	no event	Chae(2001)
1997 Nov. 3	8100	6.5	-100	17	homologous flares	Paper I
1998 Apr. 29	8210	6	30	5	M6.8 flare/CME	Paper II
1998 May 2	8210	7	90	13	X1.1 flare/CME	Paper II
1999 Aug. 16	8668	50	-300	-6	a filament formation	Paper IV
2000 June 6	9026	3.5	20	6	X2.3 flare/CME	Paper II
2000 Sep. 14	9165	96	-600	-6	several flares/CMEs	Nindos and Zhang(2002)
2000 Nov. 24	9236	22	157	7	three flares/CMEs	Paper III
2000 Nov. 25	9236	10	40	4	X1.9 flare/CME	Paper III

amount of helicity change, since the first term of Eq.(1) has not been estimated. However, it is very likely that the magnetic helicities accumulated during the observing periods play important roles in some physical process such as the occurrence of homologous flares (Paper I) and the formation of a filament in AR 8668 (Paper IV), as will be discussed more in the following subsections.

It is noted that the magnetic helicity supply by photospheric shearing motions is much larger than that by solar differential rotation, as previously demonstrated by several authors(Chae 2002; Nindos and Zhang 2002; Paper I; Paper IV). In this regard, Demoulin et al.(2002a) studied possible sources of the magnetic helicity injection into the solar corona and then concluded that differential rotation (e.g., DeVore 2000) is not efficient enough for supplying the magnetic helicity of active regions and CMEs. Demoulin et al. (2002b) further argued that photospheric shearing motions are relatively inefficient to bring magnetic helicity into the corona compared to the helicity carried by significantly twisted flux tubes. On this basis, they suggested that the contribution by emerging fluxes (first term of Eq.(1)) may be more important than that by photospheric horizontal motions (second term). Here note that they did not estimate the contribution of the shearing motions that we have estimated, which are different from differential rotation. Our results are consistent with Demoulin et al. (2002a,b) conclusion that differential rotation is not efficient. But we think it is too hasty to exclude all kinds of photospheric shearing motions from the list of possible sources of the magnetic helicity injection. Our opinion is that the relative importance between the two terms depends on an active region as well as its evolution. According to Kusano et al.(2002), both terms are comparable each other in AR 8100 in magnitude but with opposite signs.

(b) Helicity Injection Vs Flaring Flux

Using the results of Figure 1, we have examined a relationship between the helicity accumulated by photospheric horizontal motions during the flaring time interval and the integrated X-ray flux of the subsequent flare (for details, see Paper I). Figure 2 shows a strong positive correlation between two quantities. Interestingly enough, the X-ray flux increases logarithmically with the helicity deposit. This indicates that the occurrence of a series of homologous flares in NOAA AR 8100 is physically related to the accumulation of magnetic helicity in the corona by photospheric shearing motions. This observation also supports Choe & Cheng (2000) who demonstrated using resistive MHD simulations, that a series of homologous flares can be induced by continuing shearing motions. Our results strongly indicate that photospheric shearing motions did play an important role in generating the homologous flares that occurred in this active region. In addition, this correlation seems to support an "energy storage and release" model in which flaring energy is continuously stored and then released catastrophically.

Regarding the flaring time interval (waiting time) and the corresponding GOES X-ray fluxes of flares, Wheatland(2000) and Moon et al.(2001) showed that there is no clear correlation between the waiting time and the corresponding flare X-ray flux. This result was regarded to support the self-organized criticality (SOC) model of the solar corona because in a self-organized critical state the size of any output incidence is independent of the driving mode. However, our results indicates the strong positive correlation between the flare X-ray flux and the accumulated helicity for the homologous flares, which is somewhat different from the SOC picture.

(c) Impulsive Helicity Injection

As seen in Figure 1, there was an impulsive helicity injection around the peak time of GOES M4.1 flare. Figure 3 shows a comparison of photospheric horizontal velocities between before and at the peak time of the impulsive helicity injection. Major changes of the photospheric motions were found around the circled areas. This fact implies that localized shear flows are mainly responsible for the impulsive helicity injection. Figure 4 shows another example of the impulsive helicity injections associated with three X-class eruptive flares in NOAA AR 9236 (Paper III). A comparison of the helicity change rate and GOES X-ray flux shows that impulsive helicity injections occurred only around the peak times of these flares. Our studies (Paper I-III) have shown that such an impulsive helicity injection is quite common in strong flares such as X-class. So far we have found eight impulsive helicity injections near the peak times of associated flares and/or CMEs. As we did in Paper II, we decompose the time variation of the helicity change rate into two components: a smoothly varying background component $(dH/dt)_{\rm bg}$ that has a time scale longer than an hour and an impulsively varying component that has a time scale shorter than an hour. Then the helicity change contributed only by the impulsive component is obtained from the time integral

$$\Delta H_{\rm imp} = \int_{t_s}^{t_s+\Delta t} \frac{dH}{dt} - \left(\frac{dH}{dt}\right)_{\rm bg} dt, \qquad (3)$$

where t_s is the starting time of the impulsive variation and Δt is its time duration. The background component during the impulsive variation $(dH/dt)_{\rm bg}$ is approximated to be equal to the average of several background values taken just before and after the impulsive variation. Using these definitions, we summarize the characteristics of the impulsive helicity injections for the eight events in Table 2. The helicity change by the impulsive component ranges from 6 to 24×10^{40}Mx^2. These impulsive helicity changes are much less than the typical loss of magnetic helicity associated with the eruption of a CME that is about 2×10^{42} Mx^2 (Demoulin et al., 2002a). Therefore, the impulsive variation of the helicity change rate may not be important at least in the balance of magnetic helicity in active regions. Its importance may rather lie in a good possibility that it can be evidence for the dynamical coupling of flare activity in the corona and and magnetic field changes in the photosphere.

There have been several previous observations which reported sudden changes of photospheric motions and/or magnetic fields associated with solar flares. Harvey & Harvey(1976) analyzed magnetograms and Dopplergrams of MacMath region 10385 taken in the Hα and Fe I 6569 Å lines. They found oppositely moving fast velocity structures near the flaring times, particularly as the active region approaches to the limb. These vertical motions should be interpreted as strong horizontal

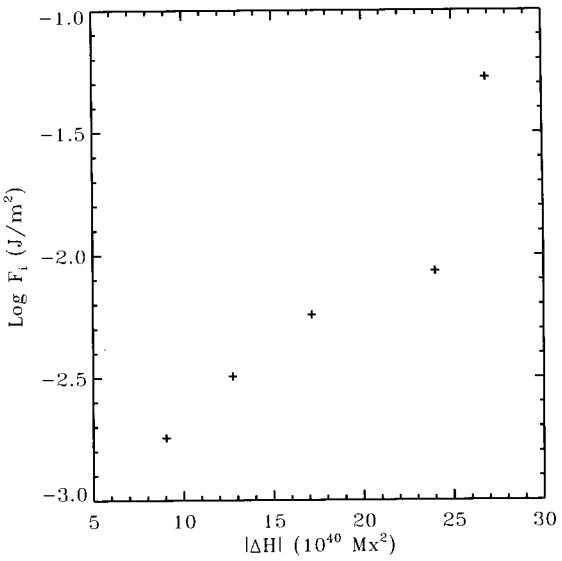

Fig. 2.— Absolute value of the magnetic helicity induced by photospheric horizontal motions accumulated during the flaring time interval vs the corresponding GOES X-ray flux integrated over the flaring time.

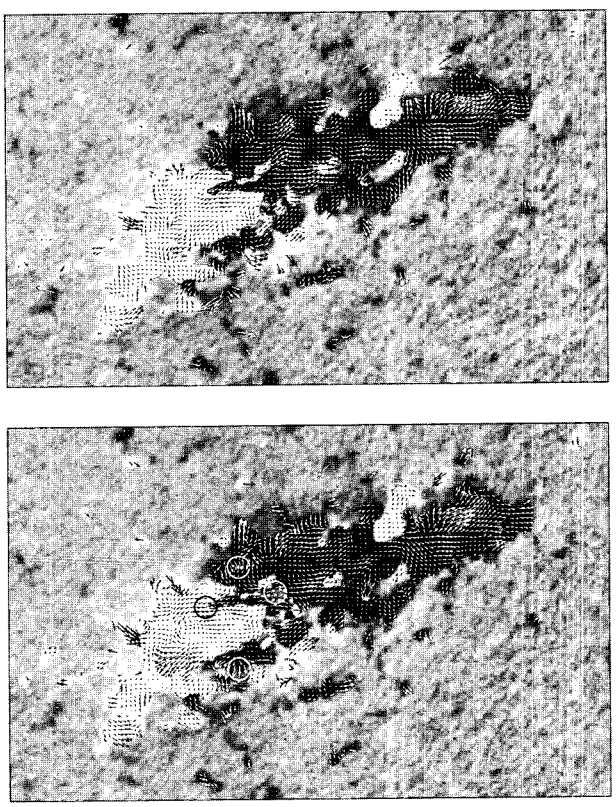

Fig. 3.— Vector maps of photospheric horizontal flows superposed on MDI magnetograms. The upper panel was taken at 02:15 UT and the lower panel taken at 02:45 UT, near the peak time of the M4.5 flare. In the lower panel, the largest arrow corresponds to 1.2 km s^{-1}.

TABLE 2
SUMMARY OF THE IMPULSIVE VARIATIONS OF MAGNETIC HELICITY.

Date	NOAA AR	Helicity Sign	X-ray[a]	$(dH/dt)_{peak}$[b] (10^{40}Mx^{2}h^{-1})	$(dH/dt)_{bg}$[c] (10^{40}Mx^{2}h^{-1})	Δt[d] (hr)	ΔH_{imp}[e] (10^{40}Mx^2)	Reference
1997 Nov. 4	8210	(−)	M4.1	-33	-15 ± 4	0.7	6	Paper I
1998 Apr. 29	8210	(+)	M6.8	-12	5 ± 2	0.7	-6	Paper II
1998 May 2	8210	(+)	X1.1	-27	15 ± 6	0.6	-15	Paper II
2000 Jun. 6	9026	(−)	X2.3	-29	15 ± 5	1.0	-23	Paper II
2000 Nov. 24	9236	(−)	X2.0	28	-10 ± 4	0.5	10	Paper III
2000 Nov. 24	9236	(−)	X2.3	45	-15 ± 4	0.5	15	Paper III
2000 Nov. 24	9236	(−)	X1.8	39	5 ± 4	0.5	8	Paper III
2000 Nov. 25	9236	(−)	X1.9	62	-15 ± 6	0.6	24	Paper II

[a]X-ray flare class observed by GOES

[b]Peak value of impulsive variation.

[c]Background value of the helicity change rate at the time of flare and the standard deviation of its temporal fluctuation.

[d]Time duration of impulsive variation.

[e]Helicity change by the impulsive component.

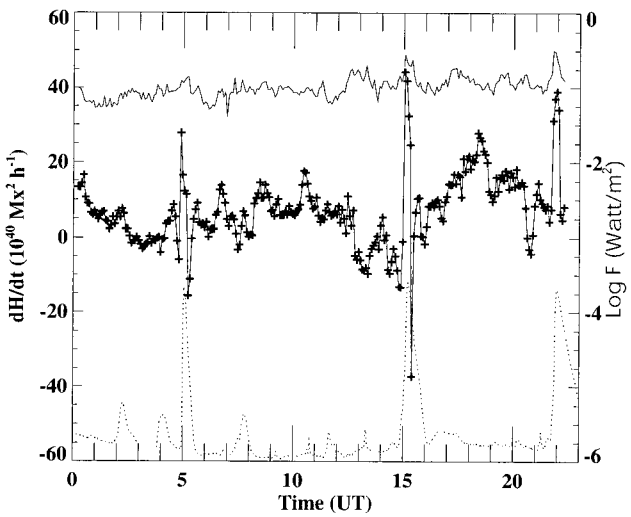

Fig. 4.— Temporal change of magnetic helicity change rate (thick solid line), GOES X-ray intensity (dotted line), and the sum of the norms of the photospheric velocity vectors (thin solid line) expressed in an arbitrary scale. The X-ray intensity is referenced to the right Y-axis.

motions when seen against the solar disk center. Anwar et al. (1993) examined proper motions of sunspots associated with an X1.5 flare occurred on 15 November 1991 and showed that the onset of a sunspot motion coincided with a rapid flare brightening. Herdwijaya et al. (1997) also examined proper motions of 276 individual sunspots and showed that about 70% of fast drift motions were related to the occurrence of flares. It should be noted that such observations of the large proper motions are never affected by the variation of spectral lines associated with flaring processes. On the other hand, Wang et al.(1994, 2002) reported impulsive and permanent increases of magnetic shear associated with X-class flares at the time scale of several minutes to one hour. Similar sudden changes associated with strong flares were also reported in linear force-free coefficients (Pevtsov et al. 1995). We summarize major results of these observations in Table 3.

(d) Helicity Injection And Filament Formation

Paper IV examined the magnetic helicity change rate of NOAA AR 8668 in which a large filament was under formation, and then found that there was a persistent pattern of shearing motions in the neighborhood of the filament. Total helicity accumulated for about 50 hours is found to be $\Delta H = -3 \times 10^{42}$ Mx^2, which is comparable to the magnetic helicity of a typical coronal mass ejection (Demoulin et al. 2002a). This result may imply that the formation of a prominence is associated

TABLE 3
PREVIOUS OTHER OBSERVATIONS RELATED TO THE IMPULSIVE HELICITY INJECTIONS

Type of Observation	Related Events	References
Strong Doppler shift	Limb flares	Harvey & Harvey (1976)
Large sunspot motions	X1.5 flare solar flares	Anwar et al.(1993) Herdiwijaya et al.(1997)
Sudden change of α[a]	strong flares	Pevtsov et al.(1995)
Abrupt increase of magnetic shear	X-class flares	Wang et al.(1994, 2002)

[a]Linear force-free coefficient

with magnetic helicity injection by shear flows, which supports Choe & Lee's (1992) work on the prominence formation.

(e) Timescales Of Shear Flows And Their Origins

Figure 4 shows different time scales of helicity injection rates which mainly originate from different types of photospheric shear flows. In Table 4, we categorize the observed shear flows into three types according to their time scales: (1) localized flows, (2) fluctuating flows, and (3) large scale flows. First, the localized shear flows whose time scale is less than 1 hour are mainly responsible for the impulsive helicity injections (for summary, see Table 2) associated with strong flare and/or CME events. One interesting question is that such an impulsive injection is a cause of a CME-flare event or its result. Regarding this question, Paper III compared the temporal variation of magnetic helicity change rate and the initial speed of a filament associated with X1.8 flare, and then found that the eruption of the filament started about 10 minutes before the impulsive variation of the helicity change rate. This fact may imply that the observed impulsive helicity change is not a cause of the eruptive solar flare but its result, i.e., photospheric response to the coronal field restructuring. A similar argument was made by Anwar et al.(1993) who estimated the magnetic force exerted to the photosphere using pre-flare and post-flare vector magnetograms. Second, the observed fluctuation flows were observed in the all active regions that we have studied. Their time scale is approximately a few hours. These flows may be related to background shear flows around the active regions. In terms of the helicity budget associated with solar eruptive events, large scale shear flows are most interesting to us. They were found in AR 8100 associated with the occurrence of homologous flares (Paper I), in AR 8668 related with a filament formation (Paper IV), and in AR 9165 which has several CME/flare events (Nindos and Zhang 2002). Their time scales are several hours for the homologous events and a couple of days for the others. Regarding their origin, Chae et al. (2003) suggested from Parker's (1974) original idea that the observed shear flows may be driven by the torque produced by the expansion of the coronal segment of a twisted flux tube that is rooted deeply below the surface. By applying a simple relation between the coronal expansion parameter and the amount of helicity transferred via shear flows to NOAA AR 8668, they found that the amount of helicity change is quantitatively consistent with the observed expansion of coronal magnetic fields seen in Yohkoh SXT images. This process may also explain the localized shear flows as a result of abrupt expansion of magnetic flux tubes associated with the initial phase of strong CME and/or flare events.

IV. SUMMARY AND FURTHER WORKS

In this paper, we have reviewed the magnetic helicity changes of several solar active regions by photospheric horizontal motions. Our results have shown that the magnetic helicity changes in the active regions are intimately associated with solar eruptive events such as flares and/or CMEs as well as the formation of a filament.

Our results that have presented in this paper are based on the estimations of the second term of Eq.(1). Recently, Kusano et al. (2002) suggested a way to determine both terms of Eq.(1) by obtaining the vertical velocity component indirectly from the induction equation, but the practicality of the method is still in debate. We are considering alternative way to determine both terms by using magnetic vectors estimated from the inversion process of full Stokes profiles and vertical velocity from their zero-shifts. For this we are analyzing polarimetric data of an active region by Advanced Stokes Polarimeter (ASP). Another plan of ours is to

TABLE 4
CLASSIFICATION OF THE OBSERVED SHEAR FLOWS RELATED TO THE MAGNETIC HELICITY INJECTIONS.

Type	Characteristic Period	Related to	References	Suggested Origin
Localized flows	Less than 1 hour	Strong flares & CMEs	Paper I-III	Photospheric response to CME-flare events
Fluctuting flows	A few hours	All regions	Paper I-IV	Background flows
Large scale flows	Hours to Several days	Homologous flares & Prominence formation	Paper I Paper IV	Helicity pumping by flux tube expansions

examine the long term evolution of magnetic helcity injection in terms of helicity balance in the solar corona: supply (from subphotosphere) and loss (via CMEs).

ACKNOWLEDGEMENTS

This paper is dedicated to Professor Hong-Sik Yun who retired his professorship at Seoul National University in February, 2003. We are very thankful to him for his sincere guidance and advice during past twenty years. We are grateful to the BBSO observing staff for their support in obtaining the data. We also thank Drs. G. S. Choe and Haimin Wang for their valuable comments and discussions. This work has been supported by NASA grants NAG5-10894 and NAG5-7837, by a MURI grant of AFOSR, by the US-Korea Cooperative Science Program (NSF INT-98-16267), by National Research Laboratory M10104000059-01J000002500 of the Korean government. SOHO is a project of international cooperation between ESA and NASA.

REFERENCES

Anwar, B., Acton, B. W., Hudson, H. S., Makita, M., McClymont, A. N., & Tsuneta, S. 1993, Rapid Sunspot Motion during a Major Flare, Sol. Phys., 147, 287

Berger, M. A., & Field, G. B. 1984, The topological properties of magnetic helicity, J. Fluid Mech., 147, 133

Burlaga, L. F. 1988, J. Geophys. Res., 93, 7217

Canfield, R. C., & Pevtsov, A. A. 1999, Helicity and reconnection in the solar corona: observations, in Magnetic Helicity in Space and Laboratory Plasmas, ed. M. R. Brown, R. C. Canfield, & A. A. Pevtsov (Geophys. Monogr. 111; Washington, DC: AGU), 197

Chae, J. 2000, The magnetic helicity sign of filament chirality, ApJ, 540, L115

Chae, J. 2001, Observational Determination of the Rate of Magnetic Helicity Transport through the Solar Surface via the Horizontal Motion of Field Line Footpoints, ApJ, 560, L95

Chae, J., Wang, H., Qiu, J., Goode, P. R., Strous, L., & Yun, H. S. 2001, The Formation of a Prominence in Active Region NOAA 8668. I. SOHO/MDI Observations of Magnetic Field Evolution, ApJ, 560, 476 (Paper IV)

Chae, J., Moon, Y.-J., Rust, D. M., Wang, H, & Goode, P. R. 2003, Magnetic helicity pumping by twisted flux tube expansion, JKAS, 36, 33

Choe, G. S. & Cheng, C. Z. 2000, A Model of Solar Flares and Their Homologous Behavior, ApJ, 541, 449

Choe, G. S. & Lee, L. C. 1992, Formation of solar prominences by photospheric shearing motions, Sol. Phys., 138, 291

Demoulin, P., Mandrini, C. H., van Driel-Gesztelyi, L., Thompson, B. J., Plunkett, S., Kovari, Zs., Aulanier, G., & Young, A. 2002a, What is the source of the magnetic helicity shed by CMEs? The long-term helicity budget of AR 7978, A&A, 382, 650

Demoulin, P., Mandrini, C. H., van Driel-Gesztelyi, L., Lopez Fuentes, M. C., & Aulanier, G. 2002b, The Magnetic Helicity Injected by Shearing Motions, Sol. Phys., 207, 87

DeVore, C. R. 2000, Magnetic helicity generation by Solar Differential Rotation, ApJ, 539, 944

Harvey, K. L. & Harvey, J. W. 1976, A study of the magnetic and velocity fields in an active region, Sol. Phys., 233, 246

Herdiwijaya, D., Makita, M., & Anwar, B. 1997, The Proper Motion of Individual Sunspots, PASJ, 49, 235

Kusano, K., T. Maeshiro, T. Yokoyama, & Sakurai, T. 2002, Measurement of magnetic helicity injection and free energy loading into the solar corona, ApJ, 577, 501

Moon, Y.-J., Choe, G. S., Yun, H. S., & Park, Y. D. 2001, Flaring time interval distribution and spatial correlation of solar major flares, J. Geophys. Res., 106, A12, 29951

Moon, Y.-J., Chae, J., Choe, G. S., Wang, H., Park, Y. D., Yun, H. S., Yurchyshyn, V. B., & Good, P. R. 2002a, Flare Activity and Magnetic Helicity Injection by Photospheric Horizontal Motions, ApJ, 574, 1066 (Paper I)

Moon, Y.-J., Chae, J., Wang, H., Choe, G. S., & Park, Y. D. 2002b, Impulsive Variations of Magnetic Helicity Change Rate associated with Eruptive Flares, ApJ, 580, 528 (Paper II)

Moon, Y.-J., Chae, J., Wang, H., & Park, Y. D. 2003, Magnetic Helicity Change Rate Associated With Three X-class Eruptive Flares, Advances in Space Research, in press (Paper III)

Nindos, A. & Zhang, H. 2002, Photospheric Motions and Coronal Mass Ejection Productivity ApJ, 573, L133

November, L. J., & Simon, G. W. 1988, Precise proper-motion measurement of solar granulation, ApJ, 333, 427

Parker, E. N. 1974, The Dynamical Properties of Twisted Ropes of Magnetic Field and the Vigor of New Active Regions on the Sun, ApJ, 191, 245

Pevtsov, A. A., Canfield, R. C., & Metcalf, T. R. 1995, Latitudinal variation of helicity of photospheric magnetic fields, ApJ, 440, L109

Pevtsov, A. A., & Canfield, R. C. 1999, Helicity of the photospheric magnetic field, in Magnetic Helicity in Space and Laboratory Plasmas, ed. M. R. Brown, R. C. Canfield, & A. A. Pevtsov (Washington, DC: AGU Geophys. Monogr. 111), 103

Rust, D. M. 1999, Magnetic helicity in solar filaments and coronal mass ejections, in Magnetic Helicity in Space and Laboratory Plasmas, ed. M. R. Brown, R. C. Canfield, & A. A. Pevtsov (Geophys. Monogr. 111; Washington, DC: AGU), 221

Scherrer, P. H., Bogart, R. S., Bush, R. I., Hoeksema, J. T., Kosovichev, A. G., Schou, J., Rosenberg, W., Springer, L., Tarbel, T. D., Title, A., Wolfson, C. J., Zayer, I, MDI Engineering Team, 1995, The Solar Oscillation Investigation - Michelson Doppler Imager, Sol. Phys., 162, 129

Wang, H., Ewell, M. W., Jr., Zirin, H., & Ai, G. 1994, Vector magnetic field changes associated with X-class flares, ApJ, 424, 436

Wang, H., Spirock, T. J., Qiu, J., Ji, H., Yurchyshyn, V. B., Moon, Y.-J., Denker, C., & Goode, P. R. 2002, Rapid Changes of Magnetic Fields Associated with Six X-class Flares, ApJ, 576, 497

Wheatland, M. S. 2000, Do Solar Flares Exhibit an Interval-size Relationship?, Sol. Phys., 191, 381